COPLANAR-WAVEGUIDE-TO-MICROSTRIP TRANSITION MODEL

Wojciech Wiatr
Institute of Electronic Systems, Warsaw University of Technology, Poland

David K. Walker and Dylan F. Williams
National Institute of Standards and Technology, Boulder, Colorado, USA

ABSTRACT

We develop a novel four-port equivalent circuit for a coplanar-waveguide-to-microstrip transition using a finite-difference time-domain analysis. The lumped model accounts for mutual inductive coupling and works well up to about 30 GHz.

INTRODUCTION

We present a finite-difference time-domain (FDTD) electromagnetic analysis of the coplanar-waveguide-to-microstrip (CPW-to-microstrip) transition shown in Fig. 1. This transition employs via holes to connect the two outer ground contacts at the substrate surface to the microstrip ground on the backside of the substrate, and is typically used to adapt microwave coplanar probes to structures embedded in the microstrip.

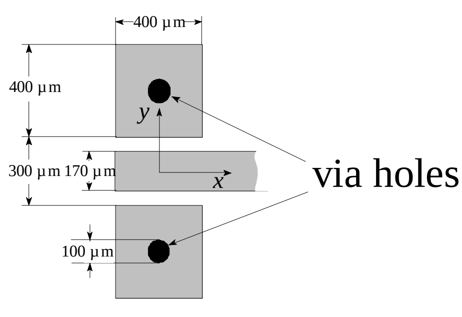

Fig. 1. Top view of transition. The center conductor also serves as the signal contact. The outer pads are connected to ground by via holes through a 175 µm thick substrate with relative dielectric constant of 10.

We used FDTD [1] to study the properties of the transition, develop a new equivalent circuit, and investigate the influence of variations of via geometry on the transition's electrical parameters.

Previous work on CPW-to-microstrip transitions focused on analyzing via-hole interconnects as discontinuities in the signal path of a microstrip line [2] or as grounds [3]. Cherry and Iskander [4] performed a more detailed study of two parallel microstrip lines coupled through interconnect vias, and developed a lumped-element equivalent circuit. We treat the transition of Fig. 1 as a general four-port circuit that includes via inductance and mutual coupling.

ANALYSIS

The transition shown in Fig. 1 can be represented generally as a four-port with three microstrip ports on the left (input) side and one microstrip port on the right (output) side. Since energy flow between these ports is caused by both magnetic and electric coupling in the vicinity of the transition, developing an equivalent circuit requires exciting these ports in several different ways.

To characterize the electrical coupling we analyzed the two different microstrip arrangements shown in Fig. 2, chosen so that the electromagnetic simulations would be symmetrical about the *x*-axis of Fig. 1. For the arrangement of Fig. 2a we applied symmetrical and anti-symmetrical stimuli sequentially to the wide ground strips at the input and placed magnetic

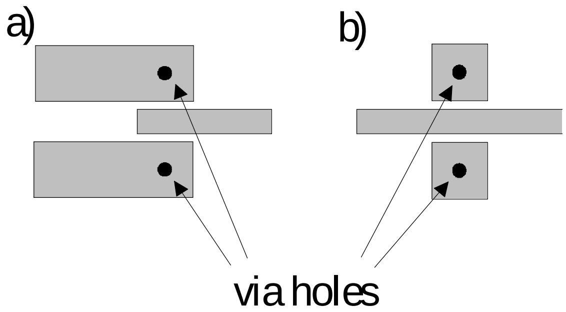

Fig. 2. Microstrip geometries used for electromagnetic simulations.

and electric walls, respectively, in the plane of symmetry to facilitate the calculations. We also terminated the left end of the central conductor in Fig. 2a with an open circuit or short circuit to ground using a thin metal strip. We excited the arrangement of Fig. 2b at the center conductor only. So, in total, we analyzed four structures; three based on that of Fig. 2a and one based on Fig. 2b. This allowed us to characterize the mutual capacitive and inductive coupling between all of the conductors.

We performed field analyses of the structures using a three-dimensional FDTD electromagnetic simulator [1]. We assumed all conductors were perfect, neglected skin effects, and substituted metal posts for the metalized via holes. We also used absorptive boundary conditions at the outer edges of the structure and applied an irregular mesh to improve the accuracy of the electromagnetic-field simulations. The reference planes for calculation of the transition scattering parameters (*S*–parameters) were set at 1.5 mm for the input and 1.1 mm for the output from the physical boundaries of the pads.

We analyzed the dependence of the *S*-parameters of the transition on small variations in via diameter and position on the pad layout. We studied five different geometries and calculated *S*-parameters in the frequency range up to 40 GHz.

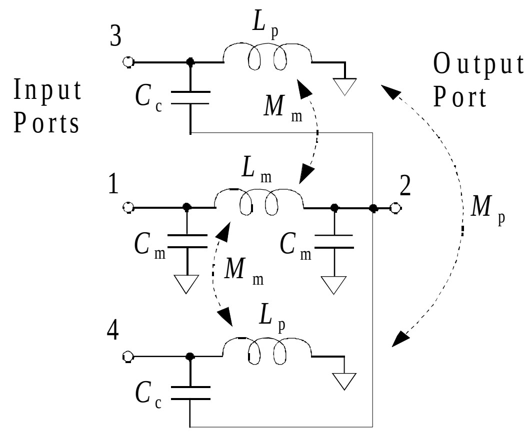

Fig. 3. Simplified lumped-element equivalent circuit for the transition.

TRANSITION MODEL

We developed the simplified lumped-element equivalent circuit model for our transition shown in Fig. 3 from our simulation results. The model is composed of two self inductances (L_p, L_m), two mutual inductances (M_m, M_p) and two capacitances (C_m, C_c).

We determined their values in our circuit with optimization procedures available in a commercial microwave circuit simulation [5]. After adding appropriate lengths of transmission line to the equivalent circuit of Fig. 3, we adjusted L_p, L_m, M_m, M_p, C_c, and C_m until the *S*-parameters of the model best matched our FDTD simulations. We accounted for the end capacitance of the open circuit and the finite inductance of the center conductor shorting strip in our model.

Using this procedure, we developed the following approximate relationships between values of the circuit components and the geometry of the interconnect pads:

$$L_m \approx 154 \text{ pH},$$

$$L_p \approx 96 \text{ pH} + (0.31 \text{ pH}/\mu\text{m})\Delta X - (47 \text{ pH})\ln(D/100\ \mu\text{m}),$$

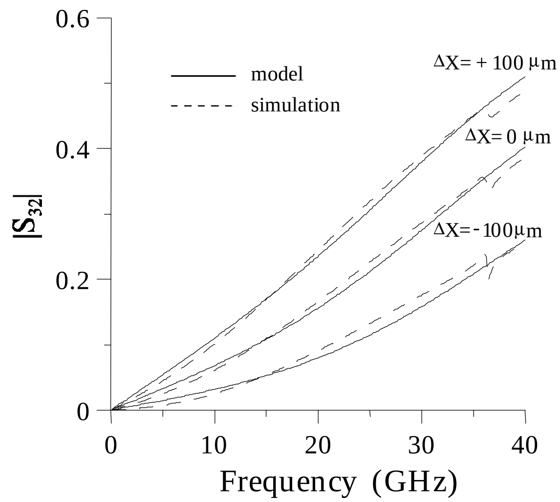

Fig. 4. Frequency dependence of S_{32} for different via positions along the x-axis in the structure of Fig. 2a excited symmetrically and the center conductor shorted to ground.

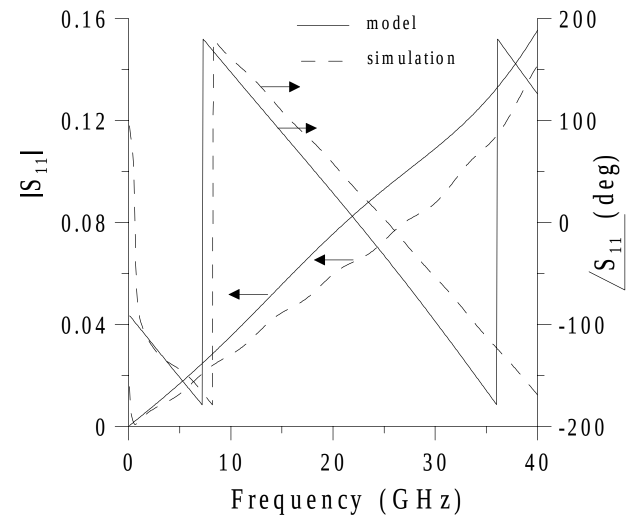

Fig. 5 Frequency dependence of S_{11} for the structure shown in Fig. 2b.

$M_m \approx$ 14.5 pH + (0.0061 pH/μm)ΔX,

$M_p \approx$ 4.8 pH + (0.02 pH/μm)ΔX,

$C_m \approx$ 33 fF, and

$C_c \approx$ 12 fF.

Here D is the via diameter and ΔX represents a change in the via hole position. We tested the formulas for values of D and ΔX up to 100 μm.

Fig. 4 compares S_{32}, the S-parameter between ports 2 and 3 as represented in Fig. 3, for the structure in Fig. 2a with symmetrical excitation for three via-hole positions along the x-axis (i.e., along the direction of the microstrip line) to the model. The three traces show effects of inductive coupling in the area between each via pad and the microstrip.

Fig. 5 shows S_{11}, the reflection coefficient looking into port 1 as represented in Fig. 3, for the structure of Fig. 2b. S_{11} increases with frequency due to inhomogeneity introduced into the microstrip line by the transition. The figures show that the model agrees well with the simulations up to about 30 GHz.

CONCLUSIONS

We studied a transition between CPW and microstrip transmission lines typically used in on-wafer measurements. Our analysis focused on the characterization of the magnetic and electric coupling in the transition.

We introduced a novel four-port equivalent circuit for the transition. It is composed of six lumped elements, including two mutual inductances and one capacitance that represent coupling in the transition. This equivalent circuit accurately models the S-parameters of the transition at frequencies up to 30 GHz. We used the model to investigate how changes in via geometry affect the transition performance and determined approximate formulas for values of the circuit elements.

REFERENCES

[1] "QuickWave 3D software manual", QWED Co., Warsaw, Poland, 1999. We use trade names to specify the experimental procedure adequately and do not imply endorsement by the National Institute of Standards and Technology. Similar products may work as well or better.

[2] J-G. Yook, N. Dib, L. Katehi, "Characterization of high frequency interconnects," *IEEE Trans. Microwave Theory Tech*., vol. MTT-42, no. 9, pp. 1727-1736, Sept. 1994.

[3] D. Koh, H. Lee, and T. Itoh, "A hybrid full-wave analysis of via-hole grounds using finite-difference and finite-element time-domain methods", *IEEE Trans. Microwave Theory Tech*., vol. MTT-45, no. 12, pp. 2217-2223, Dec. 1997.

[4] P. C Cherry, M. F. Iskander, "FDTD analysis of high frequency electronic interconnection effects," *IEEE Trans. Microwave Theory Tech*., vol. MTT-43, no. 11, pp. 2445-2451, Oct. 1995.

[5] Touchstone™ for Windows, Agilent EEsof Corp.